Inorganic Chemistry

Article

pubs.acs.org/IC

Local Coordination Geometry Perturbed β-Diketone Dysprosium Single-Ion Magnets

Jing Zhu, Changzheng Wang, Fang Luan, Tianqi Liu, Pengfei Yan, and Guangming Li*

Key Laboratory of Functional Inorganic Material Chemistry (MOE); School of Chemistry and Materials Science, Heilongjiang University, Harbin 150080, P. R. China

Supporting Information

ABSTRACT: A series of three β-diketone mononuclear dysprosium complexes, namely, $Dy(TFI)_3(H_2O)_2$ (**1**), $Dy(TFI)_3(bpy)$ (**2**), and $[Dy(TFI)_3(Phen)]\cdot 0.02CHCl_3$ (**3**) (TFI = 2-(2,2,2-trifluoroethyl)-1-indone, bpy = 2,2′-bipyridine, phen = 1,10-phenanthroline) have been designed and synthesized. Crystal structure analysis reveals that complexes **1**−**3** have haveisomorphic structures in which the central Dy(III) ion is eight-coordinated by six oxygen atoms from three TFI ligands and two O/N atoms from auxiliary ligands, forming a distorted bicapped trigonal prismatic geometry for **1**, a distorted dodecahedral geometry for **2**, and a distorted square antiprismatic geometry for **3**, respectively. Magnetic studies indicate that complex **2** with D_{2d} symmetry and **3** with D_{4d} symmetry exhibit slow magnetic relaxation with barrier heights (U_{eff}/k_B) of 48.8 K for **2** and 57.9 K for **3**. Strikingly, the relaxation time (τ) of 0.0258 s for **3** is about 20 times that for **2**, which is presumably associated with larger rotation of the SAP surroundings for **3**. Further, complexes **2** and **3** exhibit essential magnetic hysteresis loops at 1.8 K. These extend the recent reports of the single-ion magnets (SIMs) of β-diketone mononuclear dysprosium complexes.

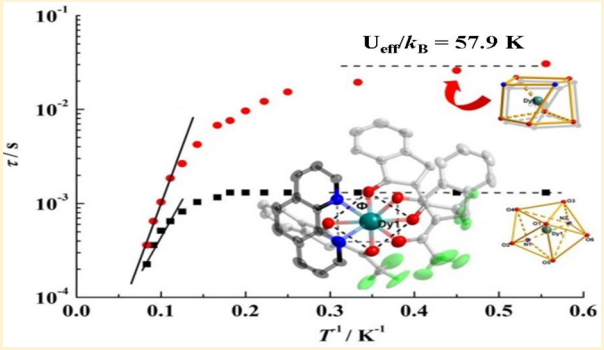

INTRODUCTION

Single-molecule magnets (SMMs) have attracted much attention due to their potential applications for the uses of high-density magnetic memories, molecular spintronics, and quantum computing devices.[1] Since the first discovery of lanthanide SMMs in 2003,[2] lanthanide ions have become fascinating candidates for constructing new SMMs, because most of them have a large orbital angular momentum, which may produce significant anisotropy to the system. Among the lanthanide ions, a large number of Dy-based SMMs of mononuclear,[3] dinuclear,[4] trinuclear,[5] tetranuclear,[6] multinuclear,[7] and chain forms[8] have been reported, attributed to the large magnetic moment with a Kramers ground state of $^6H_{15/2}$ and a large Ising-type magnetic anisotropy of Dy(III) ion. In particular, the mononuclear dysprosium complexes exhibit slow magnetization relaxation, resulting in single-ion magnets (SIMs) that have rapidly developed due to the simplification of the analysis of local anisotropy.[9] Notably, the ligand field (LF) is of importance to the magnetic anisotropy of SIMs.[10] A suitable ligand can produce a satisfactory LF, which would further dominate the riving of the ground J multiplet and result in, for the lowest sublevels, a large $|J_Z|$ and essential energy gap from the rest of the sublevels, thus realizing an magnetization easy axis. Therefore, finding a suitable ligand is one of the key factors in promoting the anisotropy barriers for Dy-based SIMs.

It is well-known that β-diketones are the most important ligands in sensitizing the luminescence of lanthanide complexes.[11] However, β-diketones have been employed to study the magnetic anisotropy[12] in recent years due to their stable bidentate chelating modes coordinating to lanthanide ions and providing suitable ligand fields.[13] For example, the groups of Gao and Tang have reported the two simple acetylacetonate (acac) complexes $[Dy(acac)_3(H_2O)_2]$[14] and $[Dy(acac)_3(phen)]$,[15] respectively, in which the metal ions exhibit Ising-type ground states with a local symmetry of D_{4d} and behave as SIMs with two anisotropy barriers of approximately 64 K. Subsequently, Tang et al. enabled the anisotropy barriers to be enhanced up to 187 K by replacing the phen with its larger aromatic derivatives.[16] However, Nojiri et al. reported that the complex $[Dy(hfac)_3(H_2O)_2]$ had a change in ligand, which has been confirmed to show practically no SMM behavior when the acac was changed to hexafluoroacetylacetonate (hfac).[17] However, a complete and detailed theoretical picture of the magnetic relaxation dynamics for the lanthanide based SIMs is still immature.

In view of recent important progress in lanthanide SMMs[12−18] as well as our longstanding research on the structures and physical properties of β-diketone lanthanide complexes,[19] a new β-diketone (2-(2,2,2-trifluoroethyl)-1-

Received: March 4, 2014
Published: August 19, 2014

dx.doi.org/10.1021/ic500501r | Inorg. Chem. 2014, 53, 8895−8901

indone) (TFI) and auxiliary ligands were employed to develop the SIMs and explore the correlation between the structure and magnetism of β-diketone lanthanide complexes. As a result, a series of three β-diketone mononuclear dysprosium complexes have been synthesized and isolated (Scheme 1). X-ray

Scheme 1. Structures of Complexes 1−3

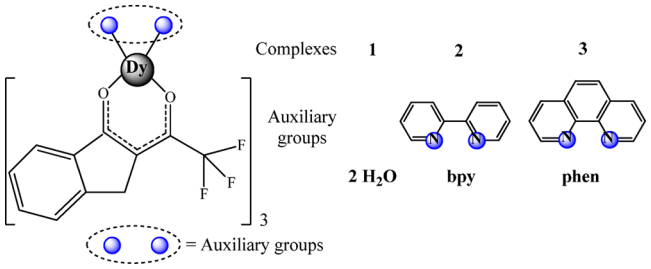

crystallographic analysis reveals that complexes **1−3** have isomorphic structures with different symmetries. Magnetic studies indicate that complex **2** with D_{2d} symmetry and complex **3** with D_{4d} symmetry exhibit slow magnetic relaxation.

EXPERIMENTAL SECTION

Materials and Instrumentation. All chemicals except $DyCl_3 \cdot 6H_2O$ and TFI were obtained from commercial sources and used without further purification. $DyCl_3 \cdot 6H_2O$ was prepared by the reaction of Dy_2O_3 and hydrochloric acid in aqueous solution. The ligand TFI was obtained by previously reported methods.[19a] Elemental (C, H, and N) analyses were conducted on a PerkinElmer 2400 analyzer. FT-IR spectra were run on a PerkinElmer 100 spectrophotometer in the range of 4000−450 cm^{-1}. UV spectra were performed on a PerkinElmer Lambda 35 spectrometer. Thermal analyses were conducted on a STA-6000 instrument in the temperature range 30−800 °C under an O_2 atmosphere. Powder X-ray diffraction (PXRD) spectra were carried out on a Rigaku D/Max-3B XRD with Cu Kα as the radiation source (λ 0.15406 nm) at room temperature in the angular range θ = 5−50°. The magnetic susceptibilities of complexes **1−3** were determined by a Quantum Design VSM magnetometer of superconducting quantum interference device (SQUID). The magnetization corrections are made by using Pascal's constants.

Synthesis of $Dy(TFI)_3(H_2O)_2$ (1). NaOH (0.088 g, 2.2 mmol) and TFI (0.50 g, 2.2 mmol) in methanol was stirred for 10 min. Then, $DyCl_3 \cdot 6H_2O$ (0.26 g, 0.71 mmol) was added dropwise to the solution and the mixture was stirred for 24 h at room temperature (Scheme S1, Supporting Information). Water was then added to the solution; a suspension was formed immediately which was then filtered to remove the suspended particles. These particles were washed with water and dried in air. Single crystals were harvested in about 2 weeks from dichloromethane/hexane. Yield: 499.8 mg (80%). Anal. Calcd for $C_{33}H_{22}DyF_9O_8$ (880.01): C, 45.04; H, 2.52. Found: C, 45.00; H, 2.58. IR (KBr, ν/cm^{-1}): 3281 (w), 1630 (s), 1501 (s), 1330 (s), 1278 (s), 1132 (s), 1039 (m), 846 (m), 753 (s). UV−vis (CH_3OH, λ_{max}/nm): 260, 343.

Synthesis of $Dy(TFI)_3(Bpy)$ (2). Complex **2** was prepared by stirring of a mixture of $Dy(TFI)_3(H_2O)_2$ (0.88 g, 1.0 mmol) and 2,2′-bipyridine (0.31 g, 2.0 mmol) in CH_3OH for 24 h at ambient temperature. The raw product was isolated according to the aforementioned method. Single crystals were obtained in about 10 days by recrystallization from chloroform/hexane. Yield: 0.87 g (87%). Anal. Calcd for $C_{43}H_{26}DyF_9N_2O_6$ (1000.16): C, 51.64; H, 2.62; N, 2.80. Found: C, 51.60; H, 2.68; N, 2.78. IR (KBr, ν/cm^{-1}): 3045 (w), 1632 (s), 1517(s), 1332 (m), 1282 (s), 1239 (m), 1130 (s), 1029 (m), 845 (m), 752 (s). UV−vis (CH_3OH, λ_{max}/nm): 259, 301, 342.

Synthesis of $[Dy(TFI)_3(Phen)] \cdot 0.02CHCl_3$ (3). Complex **3** was synthesized by stirring of a mixture of $Dy(TFI)_3(H_2O)_2$ (0.88 g, 1.0 mmol) and 1,10-phenanthroline (0.36 g, 2.0 mmol) in CH_3OH for 24 h at ambient temperature. The raw products were isolated according to the aforementioned method. Single crystals were isolated in about 10 days by recrystallization from chloroform/hexane. Yield: 0.91 g (89%). Anal. Calcd for $C_{45.02}H_{26.02}Cl_{0.06}DyF_9N_2O_6$ (1026.57): C, 52.67; H, 2.55; N, 2.73. Found: C, 52.75; H, 2.60; N, 2.72. IR (KBr, ν/cm^{-1}): 3053 (w), 1632 (s), 1516 (s), 1424 (m), 1323 (s), 1272 (s), 1207 (s), 1122 (s), 1029 (m), 845 (m), 751 (s). UV−vis (CH_3OH, λ_{max}/nm): 268, 292, 341.

X-ray Crystallography. X-ray single-crystal diffractions of complexes **1−3** were performed at 293 K on a Rigaku R-AXIS RAPID imaging plate diffractometer with graphite-monochromated Mo Kα radiation (λ = 0.71073 Å). Empirical absorption corrections on the basis of equivalent reflections were applied. The structures of **1−3** were solved by direct methods and refined with a full-matrix least-

Table 1. Crystal Data and Structure Refinement Details for Complexes 1−3

	1	2	3
empirical formula	$C_{33}H_{22}DyF_9O_8$	$C_{43}H_{26}DyF_9N_2O_6$	$C_{45.02}H_{26.02}Cl_{0.06}DyF_9N_2O_6$
formula wt	880.01	1000.16	1026.57
color	buff	buff	buff
cryst syst	monoclinic	monoclinic	monoclinic
space group	$C2/c$	$P2_1$	$P2_1/c$
a (Å)	24.059(5)	11.0539(4)	11.990(2)
b (Å)	14.993(3)	9.1328(3)	21.213(4)
c (Å)	18.366(4)	19.8252(8)	19.554(6)
α (deg)	90	90	90
β (deg)	92.54(3)	95.412(3)	116.91 (2)
γ (deg)	90	90	90
V (Å^3)	6618(2)	1992.49(13)	4434.9(18)
Z	8	2	4
ρ (g cm^3)	1.766	1.667	1.538
μ (mm^{-1})	2.359	1.968	1.774
F (000)	3448	986	2020.6
R1 ($I > 2\sigma(I)$)	0.0414	0.0427	0.0386
wR2 ($I > 2\sigma(I)$)	0.0878	0.0924	0.1129
R1 (all data)	0.0611	0.0527	0.0455
wR2 (all data)	0.0955	0.0992	0.1182
GOF on F^2	1.030	1.025	1.101

dx.doi.org/10.1021/ic500501r | Inorg. Chem. 2014, 53, 8895−8901

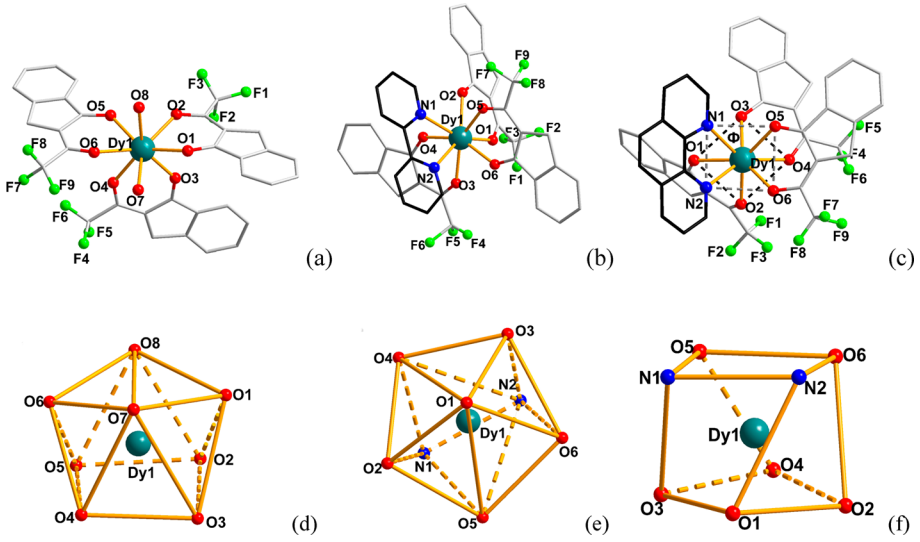

Figure 1. Molecular structures of complexes **1** (a), **2** (b), and **3** (c) and local coordination geometries of the Dy(III) ion for **1** (d), **2** (e), and **3** (f). Hydrogen atoms are omitted for clarity.

Table 2. δ (deg) and φ (deg) Values for Complexes 1−3[a]

	1		2		3				
face							SAP	TP	DD
δ_1	$O_5[O_2O_4]O_3$	9.5	$N_1[O_5N_2]O_6$	24.8	$O_6[O_5N_2]N_1$	2.5	0.0	0.0	29.5
δ_2	$O_6[O_7O_8]O_1$	23.0	$O_2[O_1O_4]O_3$	35.1	$O_4[O_3O_2]O_1$	9.1	0.0	21.8	29.5
δ_3	$O_5[O_7O_4]O_1$	52.7	$N_1[O_1N_2]O_3$	47.4	$O_6[O_3N_2]O_1$	44.9	52.4	48.2	29.5
δ_4	$O_6[O_2O_8]O_3$	40.0	$O_2[O_5O_4]O_6$	50.1	$O_4[O_5O_2]N_1$	34.6	52.4	48.2	29.5
φ_1	$O_7-O_2-O_5-O_6$	16.6	$O_4-O_5-O_3-O_6$	0.2	$O_1-O_5-O_2-O_6$	29.0	24.5	14.1	0.0
φ_2	$O_8-O_4-O_1-O_3$	14.5	$O_1-N_2-O_2-O_6$	3.2	$O_4-N_2-O_3-N_1$	24.6	24.5	14.1	0.0

[a]A[BC]D is the dihedral angle between the ABC and BCD planes. A−B−C−D is the dihedral angle between the (AB)CD and AB(CD) planes, where (AB) is the center of A and B.

squares technique.[20] All non-hydrogen atoms were refined. All crystal data and refinement parameters for complexes **1**−**3** are summarized in Table 1. The important bond lengths and angles for complexes **1**−**3** are given in Table S1 (Supporting Information). CCDC Nos. 978640, 978641, and 978642 for complexes **1**−**3**, respectively, can be obtained free of charge from the Cambridge Crystallographic Data Center via www.ccdc.cam.ac.uk/data_request/cif.

RESULTS AND DISCUSSION

Synthesis and Spectral Analysis of Complexes 1−3. Complexes **1**−**3** were prepared as shown in Scheme S1 in Supporting Information. The IR spectrum of complex **1** reveals the typical broad absorption of water molecules in complex **1** in the region 3000−3500 cm^{-1} (Figure S1, Supporting Information). In contrast, the absence of a broad band in the region 3000−3500 cm^{-1} for complexes **2** and **3** suggests that the water molecules have been substituted by the bidentate neutral donors.[21] The UV−vis spectra show that there are obviously absorption bands around 344 nm for TFI and 341 nm for complexes **1**−**3** (Figure S2, Supporting Information), which result from the singlet−singlet $\pi-\pi^*$ enol absorption of the β-diketonate. In comparison with the absorption band of TFI, the absorption maxima are blue-shifted 3 nm for complexes **1**−**3**, which result from the perturbation of the coordination of Dy(III) ion.

TG-DSC Analysis of Complexes 1−3. TG-DSC analysis (Figure S3, Supporting Information) for complex **1** exhibits a gradual weight loss of 4% in the first step, 95−155 °C, which corresponds to the loss of the crystalline water molecules (calcd 4.1%), and then it undergoes a single-step decomposition. In contrast, complexes **2** and **3** are more stable than complex **1**, meaning that there are no solvents in complexes **2** and **3** (Figure S4 and S5, Supporting Information).

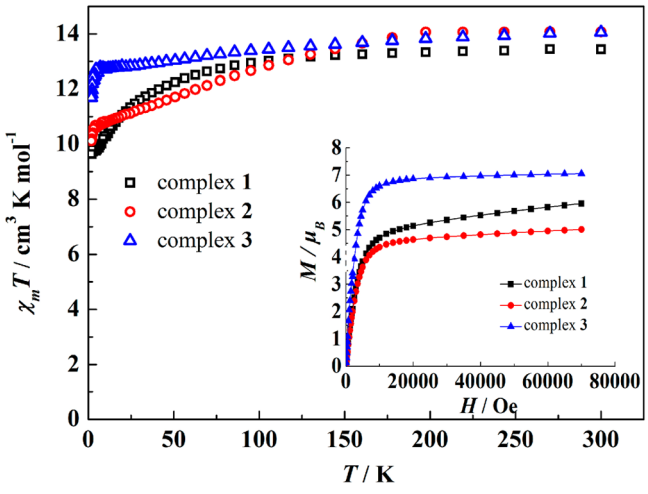

Figure 2. Temperature dependence of $\chi_m T$ at 100 Oe for **1**−**3** in the range 1.8−300 K. Inset: field dependence of magnetization for complexes **1**−**3** at 1.8 K.

PXRD Analysis of Complexes 1−3. Powder X-ray diffraction (PXRD) patterns of complexes **1**−**3** are in

dx.doi.org/10.1021/ic500501r | Inorg. Chem. 2014, 53, 8895−8901

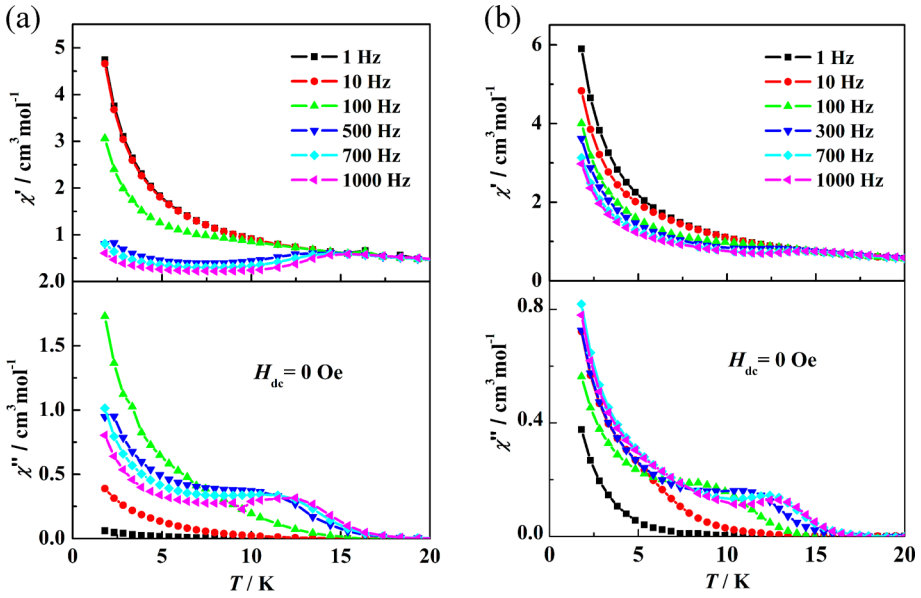

Figure 3. Temperature dependence of the in-phase (χ') and out-of-phase (χ'') ac susceptibilities under 0 Oe in the frequency range 1−1000 Hz for complexes **2** (a) and **3** (b).

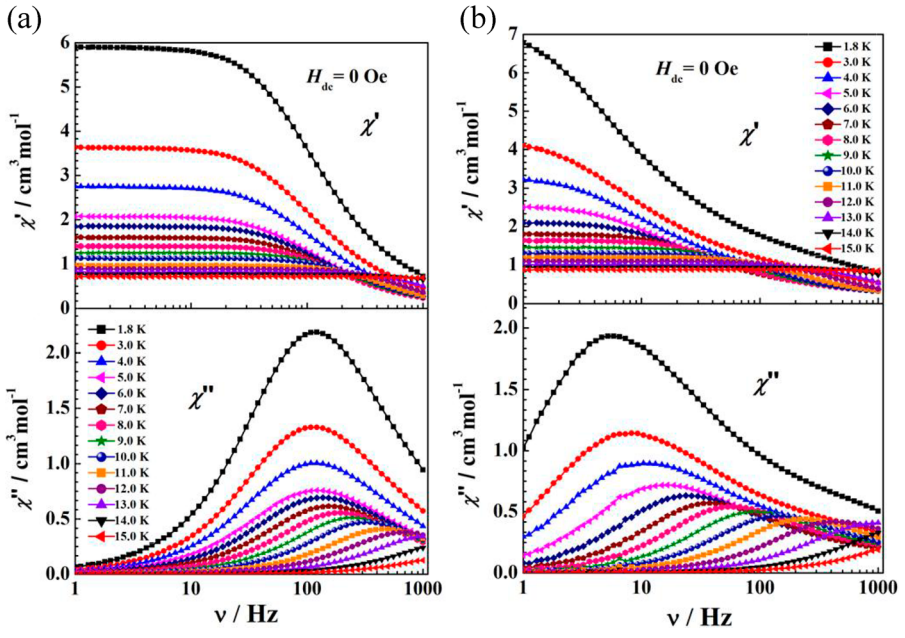

Figure 4. Frequency dependence of the in-phase (χ') and out-of-phase (χ'') ac susceptibility under 0 Oe in the temperature range 1.8−15 K for complexes **2** (a) and **3** (b).

agreement with the simulated patterns (Figures S6−S8, Supporting Information). PXRD analysis further demonstrates that the crystal structures of complexes **1**−**3** are truly representative of the bulk materials. The differences in intensity are due to the preferred orientation of the powder samples.

Structural Descriptions of 1−3. Crystal structure analysis suggests that all complexes **1**−**3** are mononuclear. The structure of complex **1** is in the monoclinic space group *C*2/*c*. The Dy1(III) ion is eight-coordinated by two oxygen atoms from two H_2O molecules and six oxygen atoms from three TFI ligands (Figure 1a). The average Dy−O (TFI oxygen atoms) bond length is 2.350 Å, which is slightly shorter than the averge Dy−O (water oxygen atom, 2.410 Å) distances. The Dy-$(TFI)_3(H_2O)_2$ molecules are stacked by $\pi-\pi$ and hydrogen bonds with the shortest Dy···Dy distances of 5.732 Å (Figure S9, Supporting Information). In contrast, complexes **2** and **3** crystallize in space groups $P2_1$ and $P2_1/c$, respectively. In the typical structures of complexes **2** and **3** (Figure 1b,c), two H_2O molecules are replaced by the ligands of bpy and phen, in which each central Dy(III) ion is coordinated by two nitrogen atoms from the bpy or phen ligand and six oxygen atoms from three TFI ligands, respectively. The average Dy−N (2.566 Å) and Dy−O (2.337 Å) bond distances in complex **2** are longer than those in complex **3**, where the average Dy−N and Dy−O bond distances are 2.531 and 2.336 Å, respectively. It is notable that the intermolecular forces in **2** and **3** are different. There are only hydrogen bonds in **2** (Figure S10, Supporting Information), while both hydrogen bonds and $\pi-\pi$ stacking

dx.doi.org/10.1021/ic500501r | Inorg. Chem. 2014, 53, 8895−8901

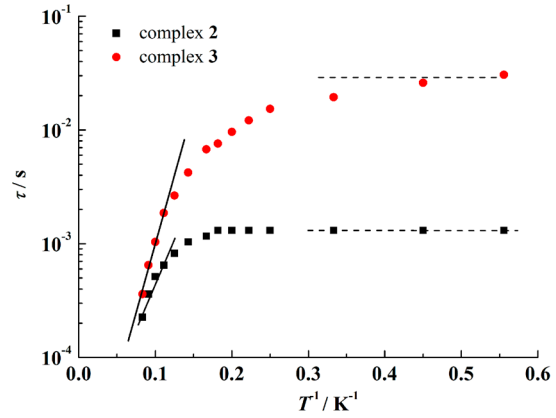

Figure 5. Temperature dependence of the relaxation times for **2** (squares) and **3** (circles) under 0 dc field. The solid lines represent linear fits of the Arrhenius law for **2** and **3**, respectively, while the dashed lines indicate the QT times.

exist in **3** (Figure S11, Supporting Information). The shortest Dy···Dy distances between the two molecules are 9.133 Å for **2** and 10.431 Å for **3**.

Notably, the coordination geometries of the Dy(III) ion in complexes **1**−**3** are different, although they are all eight-coordinated. According to the semiquantitative method of polytopal analysis,[22] the coordination geometries of Dy(III) ion for complexes **1**−**3** can be definited as a distorted bicapped trigonal prism (Figure 1d), dodecahedron (Figure 1e), and square antiprism (Figure 1f), respectively. Relevant dihedral angles for complexes **1**−**3** are summarized in Table 2, in which δ_1 and δ_2 represent the planarity of the squares and δ_3 and δ_4 the triangular faces. For complex **1**, the δ_1−δ_4 and φ_1−φ_2 values are 9.5, 23.0, 40.0, 52.7° and 16.6, 14.5°, which are close to the angles (0.0, 21.8, 48.2, 48.2° and 14.1, 14.1°) of an ideal bicapped trigonal prism. For complex **2**, the δ_1−δ_4 and φ_1−φ_2 values are 24.8, 35.1, 47.4, 50.1° and 0.2, 3.2°, which are relatively close to the angles (29.5, 29.5, 29.5, 29.5° and 0.0, 0.0°) of an ideal dodecahedron, indicative of D_{2d} symmetry. For complex **3**, the δ_1−δ_4 and φ_1−φ_2 values are 2.5, 9.1, 44.9, 34.6° and 29.0, 24.6°, which are relatively close to the angles (0.0, 0.0, 52.4, 52.4° and 24.5, 24.5°) of an ideal square antiprism, indicative of D_{4d} symmetry.

Magnetic Properties. Direct current (dc) magnetic susceptibility studies suggest the $\chi_m T$ values at room temperature are 13.9, 13.6, and 14.0 cm^3 K mol^{-1} for **1**−**3** (Figure 2), respectively, which are close to the value of 14.17 cm^3 K mol^{-1} for a single Dy(III) ion ($^6H_{15/2}$, S = 5/2, L = 5, g = 4/3, C = 14.17 cm^3 K mol^{-1}). For complex **1**, the $\chi_m T$ value reduced smoothly along with the temperature reduction in the whole temperature range of 300−1.8 K.[23] However, the curves for complexes **2** and **3** are much different from that of **1**. For example, the $\chi_m T$ value reduced smoothly along with the temperature reduction from 300 to 12 K for **2** and 20 K for **3**. Then the $\chi_m T$ value suddenly reduced to 10.24 and 11.69 cm^3 K mol^{-1} at 1.8 K for **2** and **3**, respectively. This phenomenon results from the different crystal fields around the Dy(III) ions in complexes **1**−**3**.[5d]

On the basis of the M−H curves for complexes **1**−**3** (Figure 2, inset), the magnetization at 1.8 K from zero dc field to 70 kOe reached the maxims of 6.0, 5.0, and 7.1 μ_B for complexes **1**−**3**, respectively, which are obviously lower than the calculated values for one uncorrelated Dy(III) magnetic moments ($g_J \times J$ = 4/3 × 15/2 = 10 μ_B). It is highly likely due to the crystal-field effect on the Dy(III) ion that eliminates the degeneracy of the $^6H_{15/2}$ ground state.[12b] The nonsuperimposition of the M versus H/T curves on a single curve reveals the existence of low-lying excited states and/or significant magnetic anisotropy in complexes **1**−**3** (Figure S12, Supporting Information).[24]

The ac magnetic susceptibilities for **2** and **3** (Figure 3 and Figure S13, Supporting Information) reveal that the ac susceptibilities under zero dc field are frequency dependent for **2** and **3** but not for **1** (Figure S13, Supporting Information). Such a phenomenon is similar to that for the reported analogues [Dy(hafc)$_3$(H$_2$O)$_2$][17] and [Dy(hafc)$_3$(bpy)$_2$],[12b] in which the magnetic behavior changed from non frequency dependent to frequency dependent when H$_2$O molecules in [Dy(hafc)$_3$(H$_2$O)$_2$] were replaced by bpy in [Dy(hafc)$_3$(bpy)$_2$].

Further, ac susceptibility curves for complexes **2** and **3** (Figure 4) show obvious temperature and frequency dependence in the signal of spin "freezing" by the anisotropy barriers. The χ'' values also show a maximum at 11 K (500 Hz)−12.5 K (1500 Hz) for **2** and 8 K (100 Hz)−13 K (1500 Hz) for **3** (Figure 3). Thus, the peaks of ac magnetic susceptibility in the low-temperature region suggest that **2** and **3** are typical SIMs. Upon further cooling, the χ'' values increase below 7 K, which result from the quantum tunneling effects at zero dc field. This is in agreement with values for those previously reported SIMs.[9]

According to the ac susceptibility of frequency and the temperature dependence between 1.8 and 12 K, the magnetic dynamics of **2** and **3** become temperature independent below 8

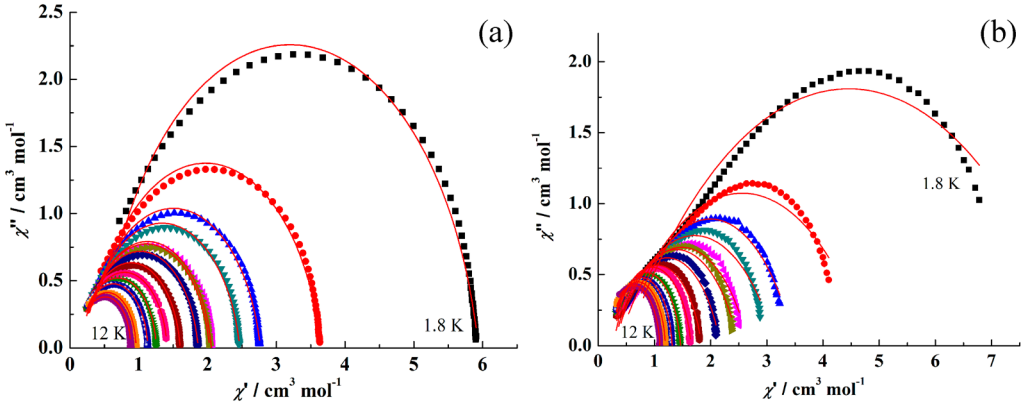

Figure 6. Cole−Cole plots measured at 1.8−12 K in 0 dc field for **2** (a) and **3** (b).

dx.doi.org/10.1021/ic500501r | Inorg. Chem. 2014, 53, 8895−8901

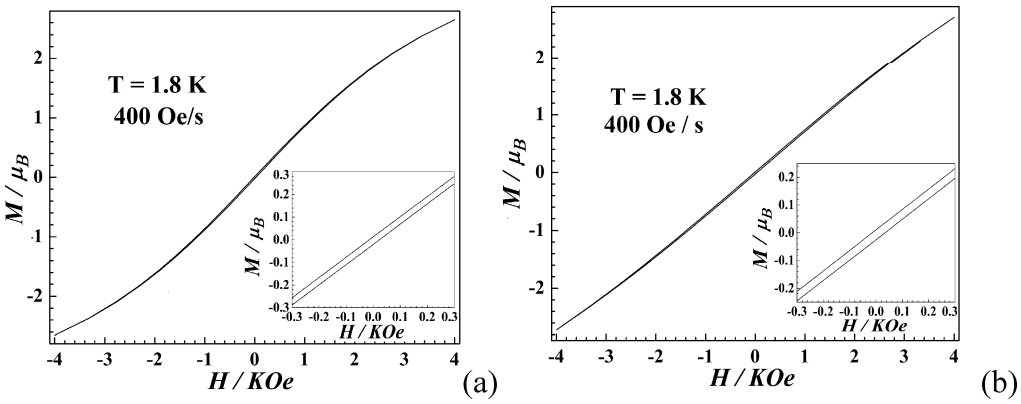

Figure 7. Hysteresis loop for complexes **2** (a) and **3** (b) at 1.8 K.

K as expected in a pure quantum regime with magnetization relaxation times (τ) of 0.0013 s for **2** and 0.0258 s for **3** (Figure 5). Notably, the relaxation time of complex **3** is longer than that previously reported for the pure β-diketone dysprosium analogue.[9,14−16] On the basis of the Arrhenius relation ($\tau = \tau_0 \exp(U_{eff}/k_BT)$), the magnetic energy barriers (U_{eff}/k_B) and the pre-exponential factors (τ_0) have been fitted at 48.8 K and 3.99×10^{-6} s as well as at 57.9 K and 3.10×10^{-6} s for **2** and **3**, respectively. Obviously, the barrier height (U_{eff}/k_B) for **3** is higher than that for **2**, which may be attributed to two factors. (i) The large aromatic SAP ligand field of phen around the Dy(III) ion in complex **3** enables the lowest doubly degenerate sublevels (formally pertaining to the large J_z values of ±11/2 or ±13/2 for dysprosium in the SAP environment[1b]) essentially separated from the rest of the substates, which results in a strong uniaxial magnetic anisotropy and higher thermal barrier.[16] (ii) The changes of the screw axis from 2-fold of complex **2** to 4-fold of complex **3**, possibly strengthening the magnetic anisotropy of Dy(III) ions, further enhances the magnetic anisotropy of Dy(III) ions from **2** to **3**.[12b,17] Strikingly, the energy barriers for complexes **2** and **3** are higher than those for the previously reported β-diketone Dy(III) analogues $Dy(hafc)_3(bpy)_2$][13b] and [$Dy(NTA)_3L$] (L = (1*R*,2*R*)-1,2-diphenylethane-1,2-diamine)[12e] but lower than those of the series of acetylacetonate Dy(III) analogues[14−16] [$Dy(acac)_3(H_2O)_2$], [$Dy(acac)_3(phen)$], and [$Dy(TTA)_3L$] (L = bpy, phen).[9]

To examine the quantum tunneling effect, the ac susceptibility measurements were further conducted under a static dc field of 2000 Oe (Figure S14, Supporting Information). The magnetic susceptibilities of out-of-phase (χ'') and in-phase forms (χ') are frequency dependent with the full peaks from 1 to 1000 Hz for complexes **2** and **3**. This suggests that the quantum tunneling effect is suppressed by an increase in the dc field. In addition, the maxima of the magnetic susceptibility shift to high temperature with increasing frequency, revealing that the low-frequency peaks occur in the lower temperature region, which is the nature of a superparamagnet.[12−18] Unfortunately, this phenomenon did not still appear for complex **1** (Figure S14a, Supporting Information).

On the basis of the frequency dependence of the ac susceptibility, the Cole−Cole plots can be simulated to the generalized Debye model.[25] The α_{Cole} values are 0.126 at 1.8 K and 0.003 at 12 K for **2** (Figure 6a and Table S2, Supporting Information). This indicates that a mainly single relaxation is involved in the present relaxation process. While the α_{Cole} parameters of **3** are 0.456 at 1.8 K and 0.065 at 12 K (Figure 6b and Table S3, Supporting Information), which suggests that two relaxation processes may be involved in the whole temperature range, such a behavior has suggested that the tunneling relaxation process is more susceptible to the local geometries or disorder than the thermally activated process.[16,26]

It is known that magnetic hysteresis is another important characteristic of the magnetic bistability of SMMs. When the dc magnetism is performed at 1.8 K with a sweep rate of 400 Oe/s, the $M-H$ curves exhibit a very narrow hysteresis loop for complexes **2** and **3** within ±4 kOe (Figure 7). Furthermore, much narrower hysteresis loops can be observed for complexes **2** and **3** within ±4 kOe (Figure S15, Supporting Information) upon slowing down the sweep rate to 50 and 200 Oe/s at 1.8 K. This further suggests that complexes **2** and **3** are SIMs and the magnetic hysteresis for complexes **2** and **3** are sweep rate dependent, which are similar to the case for previously reported Dy systems.[8a]

■ CONCLUSIONS

We have designed and isolated a series of three β-diketone mononuclear dysprosium complexes by employing a new β-diketone (TIF) and auxiliary ligands (bpy and phen). Structural analysis reveals that the auxiliary ligands play an essential role in controlling the coordination geometries of the Dy(III) ions with different symmetries. The local coordination geometries and the ligand fields of Dy(III) ions are attributed to single-ion magnets for complexes **2** and **3** but not for complex **1**. The higher symmetry and the relatively large aromatic SAP ligand (phen) result in the considerably high energy barrier of 57.8 K and a longer magnetization relaxation time of 0.0258 s of complex **3** among the β-diketone lanthanide analogues. The hysteresis loop observed at 1.8 K further certifies that complexes **2** and **3** are SIMs. This approach provided a facial route to develop the SIMs of β-diketone lanthanide complexes by adjusting the coordination geometry through the replacement of the auxiliary ligands.

■ ASSOCIATED CONTENT

Ⓢ Supporting Information

Figures, tables, and CIF files giving X-ray crystallographic data for complexes **1**−**3**, additional FT-IR spectra, UV spectra, TG-DSC analysis, powder X-ray diffraction, crystal structures, and magnetic characterization data for complexes **1**−**3**, selected bond lengths and angles for complexes **1**−**3**, and fitted parameters of the Cole−Cole plots for complexes **2** and **3** at

dx.doi.org/10.1021/ic500501r | Inorg. Chem. 2014, 53, 8895−8901

H_{dc}= 0 G. This material is available free of charge via the Internet at http://pubs.acs.org.

AUTHOR INFORMATION

Corresponding Author

*E-mail: gmli_2000@163.com.

Notes

The authors declare no competing financial interest.

ACKNOWLEDGMENTS

This work was financially supported by the National Natural Science Foundation of China (No. 51272069).

REFERENCES

(1) (a) Woodruff, D. N.; Winpenny, R. E. P.; Layfield, R. A. *Chem. Rev.* **2013**, *113*, 5110−5148. (b) Sorace, L.; Benelli, C.; Gatteschi, D. *Chem. Soc. Rev.* **2011**, *40*, 3092−3104. (c) Bogani, L.; Wernsdorfer, W. *Nat. Mater.* **2008**, *7*, 179−186. (d) Yamanouchi, M.; Chiba, D.; Matsukura, F.; Ohno, H. *Nature* **2004**, *428*, 539−542.

(2) Ishikawa, N.; Sugita, M.; Ishikawa, T.; Koshihara, S.; Kaizu, Y. *J. Am. Chem. Soc.* **2003**, *125*, 8694−8695.

(3) (a) Jiang, S. D.; Wang, B. W.; Sun, H. L.; Wang, Z. M.; Gao, S. *J. Am. Chem. Soc.* **2011**, *133*, 4730−4733. (b) AlDamen, M. A.; Cardona-Serra, S.; Clemente-Juan, J. M.; Coronado, E.; Gaita-Ariño, A.; Martí-Gastaldo, C.; Luis, F.; Montero, O. *Inorg. Chem.* **2009**, *48*, 3467−3479. (c) AlDamen, M. A.; Clemente-Juan, J. M.; Coronado, E.; Martí-Gastaldo, C.; Gaita-Ariño, A. *J. Am. Chem. Soc.* **2008**, *130*, 8874−8875.

(4) (a) Zhao, L.; Wu, J. F.; Ke, H. S.; Tang, J. K. *CrystEngComm* **2013**, *15*, 5301−5306. (b) Guo, Y. N.; Xu, G. F.; Wernsdorfer, W.; Ungur, L.; Guo, Y.; Tang, J. K.; Zhang, H. J.; Chibotaru, L. F.; Powell, A. K. *J. Am. Chem. Soc.* **2011**, *133*, 11948−11951. (c) Guo, Y. N.; Chen, X. H.; Xue, S. F.; Tang, J. K. *Inorg. Chem.* **2011**, *50*, 9705−9713. (d) Habib, F.; Lin, P. H.; Long, J.; Korobkov, I.; Wernsdorfer, W.; Murugesu, M. *J. Am. Chem. Soc.* **2011**, *133*, 8830−8833.

(5) (a) Shen, S.; Xue, S. F.; Lin, S. Y.; Zhao, L.; Tang, J. K. *Dalton Trans.* **2013**, *42*, 10413−10416. (b) Lin, S. Y.; Zhao, L.; Guo, Y. N.; Zhang, P.; Guo, Y.; Tang, J. K. *Inorg. Chem.* **2012**, *51*, 10522−10528. (c) Hewitt, I. J.; Lan, Y. H.; Anson, C. E.; Luzon, J.; Sessoli, R.; Powell, A. K. *Chem. Commun.* **2009**, 6765−6767. (d) Tang, J. K.; Hewitt, I.; Madhu, N. T.; Chastanet, G.; Wernsdorfer, W.; Anson, C. E.; Benelli, C.; Sessoli, R.; Powell, A. K. *Angew. Chem., Int. Ed.* **2006**, *45*, 1729−1733.

(6) (a) Jami, A. K.; Baskar, V.; Sañudo, E. C. *Inorg. Chem.* **2013**, *52*, 2432−2438. (b) Guo, P. H.; Liu, J. L.; Zhang, Z. M.; Ungur, L.; Chibotaru, L. F.; Leng, J. D.; Guo, F. S.; Tong, M. L. *Inorg. Chem.* **2012**, *51*, 1233−1235. (c) Zheng, Y. Z.; Lan, Y. H.; Anson, C. E.; Powell, A. K. *Inorg. Chem.* **2008**, *47*, 10813−10815.

(7) (a) Xu, X. B.; Zhao, L.; Xu, G. F.; Guo, Y. N.; Tang, J. K.; Liu, Z. L. *Dalton Trans.* **2011**, *40*, 6440−6444. (b) Li, X. L.; He, L. F.; Feng, X. L.; Song, Y.; Hu, M.; Han, L. F.; Zheng, X. J.; Zhang, Z. H.; Fang, S. M. *CrystEngComm* **2011**, *13*, 3643−3645. (c) Hussain, B.; Savard, D.; Burchell, T. J.; Wernsdorfer, W.; Murugesu, M. *Chem. Commun.* **2009**, 1100−1102. (d) Ke, H. S.; Xu, G. F.; Zhao, L.; Tang, J. K.; Zhang, X. Y.; Zhang, H. J. *Chem. Eur. J.* **2009**, *15*, 10335−10338.

(8) (a) Thielemann, D. T.; Klinger, M.; Wolf, T. J. A.; Lan, Y. L.; Wernsdorfer, W.; Busse, M.; Roesky, P. W.; Unterreiner, A.-N.; Powell, A. K.; Junk, P. C.; Deacon, G. B. *Inorg. Chem.* **2011**, *50*, 11990−12000. (b) Wang, Y.; Li, X. L.; Wang, T. W.; Song, Y.; You, X. Z. *Inorg. Chem.* **2010**, *49*, 969−976.

(9) Bi, Y.; Guo, Y. N.; Zhao, L.; Guo, Y.; Lin, S. Y.; Jiang, S. D.; Tang, J. K.; Wang, B. W.; Gao, S. *Chem. Eur. J.* **2011**, *17*, 12476−12481.

(10) (a) Takamatsu, S.; Ishikawa, T.; Koshihara, S. Y.; Ishikawa, N. *Inorg. Chem.* **2007**, *46*, 7250−7252. (b) Li, D. P.; Wang, T. W.; Li, C. H.; Liu, D. S.; Li, Y. Z.; You, X. Z. *Chem. Commun.* **2010**, *46*, 2929−2931.

(11) (a) Lima, P. P.; Nolasco, M. M.; Paz, F. A. A.; Ferreira, R. A. S.; Longo, R. L.; Malta, O. L.; Carlos, L. D. *Chem. Mater.* **2013**, *25*, 586−598. (b) Shi, J.; Hou, Y. J.; Chu, W. Y.; Shi, X. H.; Gu, H. Q.; Wang, B. L.; Sun, Z. Z. *Inorg. Chem.* **2013**, *52*, 5013−5022. (c) Sun, W.; Yu, J. B.; Deng, R. P.; Rong, Y.; Fujimoto, B.; Wu, C. F.; Zhang, H. J.; Chiu, D. T. *Angew. Chem., Int. Ed.* **2013**, *52*, 1−5. (d) Zhou, S. S.; Xue, X.; Wang, J. F.; Dong, Y.; Jiang, B.; Wei, D.; Wan, M. L.; Jia, Y. *J. Mater. Chem.* **2012**, *22*, 22774−22780.

(12) (a) Chilton, N. F.; Langley, S. K.; Moubaraki, B.; Soncini, A.; Batten, S. R.; Murray, K. S. *Chem. Sci.* **2013**, *4*, 1719−1730. (b) Wang, Y. L.; Ma, Y.; Yang, X.; Tang, J. K.; Cheng, P.; Wang, Q. L.; Li, L. C.; Liao, D. Z. *Inorg. Chem.* **2013**, *52*, 7380−7386. (c) Liu, C. M.; Zhang, D. Q.; Zhu, D. B. *Inorg. Chem.* **2013**, *52*, 8933−8940. (d) Sun, W. B.; Han, B. L.; Lin, P. H.; Li, H. F.; Chen, P.; Tian, Y. M.; Murugesu, M.; Yan, P. F. *Dalton Trans.* **2013**, *42*, 13397−13403. (e) Li, D. P.; Zhang, X. P.; Wang, T. W.; Ma, B. B.; Li, C. H.; Li, Y. Z.; You, X. Z. *Chem. Commun.* **2011**, *47*, 6867−6869.

(13) (a) Bernot, K.; Luzon, J.; Bogani, L.; Etienne, M.; Sangregorio, C.; Shanmugam, M.; Caneschi, A.; Sessoli, R.; Gatteschi, D. *J. Am. Chem. Soc.* **2009**, *131*, 5573−5579. (b) Ma, Y.; Xu, G. F.; Yang, X.; Li, L. C.; Tang, J. K.; Yan, S. P.; Cheng, P.; Liao, D. Z. *Chem. Commun.* **2010**, *46*, 8264−8266.

(14) Jiang, S. D.; Wang, B. W.; Su, G.; Wang, Z. M.; Gao, S. *Angew. Chem., Int. Ed.* **2010**, *49*, 7448−7451.

(15) Chen, G. J.; Gao, C. Y.; Tian, J. L.; Tang, J. K.; Gu, W.; Liu, X.; Yan, S. P.; Liao, D. Z.; Cheng, P. *Dalton Trans.* **2011**, *40*, 5579−5583.

(16) Chen, G.; Guo, Y.; Tian, J.; Tang, J.; Gu, W.; Liu, X.; Yan, S.; Cheng, P.; Liao, D. Z. *Chem. Eur. J.* **2012**, *18*, 2484−2487.

(17) Mori, F.; Nyui, T.; Ishida, T.; Nogami, T.; Choi, K. Y.; Nojiri, H. *J. Am. Chem. Soc.* **2006**, *128*, 1440−1441.

(18) (a) Roy, J. J. L.; Jeletic, M.; Gorelsky, S. I.; Korobkov, I.; Ungur, L.; Chibotaru, L. F.; Murugesu, M. *J. Am. Chem. Soc.* **2013**, *135*, 3502−3510. (b) Liu, J. L.; Yuan, K.; Leng, J. D.; Ungur, L.; Wernsdorfer, W.; Guo, F. S.; Chibotaru, L. F.; Tong, M. L. *Inorg. Chem.* **2012**, *51*, 8538−8544. (c) Cardona-Serra, S.; Clemente-Juan, J. M.; Coronado, E.; Gaita-Ariño, A.; Camón, A.; Evangelisti, M.; Luis, F.; Martínez-Pérez, M. J.; Sesé, J. *J. Am. Chem. Soc.* **2012**, *134*, 14982−14990.

(19) (a) Li, J. Y.; Li, H. F.; Yan, P. F.; Chen, P.; Hou, G. F.; Li, G. M. *Inorg. Chem.* **2012**, *51*, 5050−5057. (b) Li, W. Z.; Yan, P. F.; Hou, G. F.; Li, H. F.; Li, G. M. *Dalton Trans.* **2013**, *42*, 11537−11547. (c) Li, W. Z.; Yan, P. F.; Hou, G. F.; Li, H. F.; Li, G. M. *RSC Adv.* **2013**, *3*, 18173−18180. (d) Li, H. F.; Yan, P. F.; Chen, P.; Wang, Y.; Xu, H.; Li, G. M. *Dalton Trans.* **2012**, *41*, 900−907.

(20) Sheldrick, G. M. *Acta Crystallogr., Sect. A* **2008**, *64*, 112−122.

(21) (a) De Silva, C. R.; Maeyer, J. R.; Wang, R. Y.; Nichol, G. S.; Zheng, Z. P. *Inorg. Chim. Acta* **2007**, *360*, 3543−3552. (b) Bellusci, A.; Barberio, G.; Crispini, A.; Ghedini, M.; Deda, M. L.; Pucci, D. *Inorg. Chem.* **2005**, *44*, 1818−1825.

(22) (a) Mei, X. L.; Ma, Y.; Li, L. C.; Liao, D. Z. *Dalton Trans.* **2012**, *41*, 505−511. (b) Muetterties, E. L.; Guggenberger, L. J. *J. Am. Chem. Soc.* **1974**, *96*, 1748−1756.

(23) (a) Kahn, M. L.; Ballou, R.; Porcher, P.; Kahndagger, O.; Sutter, J.-P. *Chem. Eur. J.* **2002**, *8*, 525. (b) Kahn, M. L.; Sutter, J.-P.; Golhen, S.; Guionneau, P.; Ouahab, L.; Kahn, O.; Chasseau, D. *J. Am. Chem. Soc.* **2000**, *122*, 3413−3421.

(24) Abbas, G.; Lan, Y. H.; Kostakis, G. E.; Wernsdorfer, W.; Anson, C. E.; Powell, A. K. *Inorg. Chem.* **2010**, *49*, 8067−8072.

(25) Aubin, S. M. J.; Sun, Z.; Pardi, L.; Krzystek, J.; Folting, K.; Brunel, L. C.; Rheingold, A. L.; Christou, G.; Hendrickson, D. N. *Inorg. Chem.* **1999**, *38*, 5329−5340.

(26) Bernot, K.; Pointillart, F.; Rosa, P.; Etienne, M.; Sessoli, R.; Gatteschi, D. *Chem. Commun.* **2010**, *46*, 6458−6460.